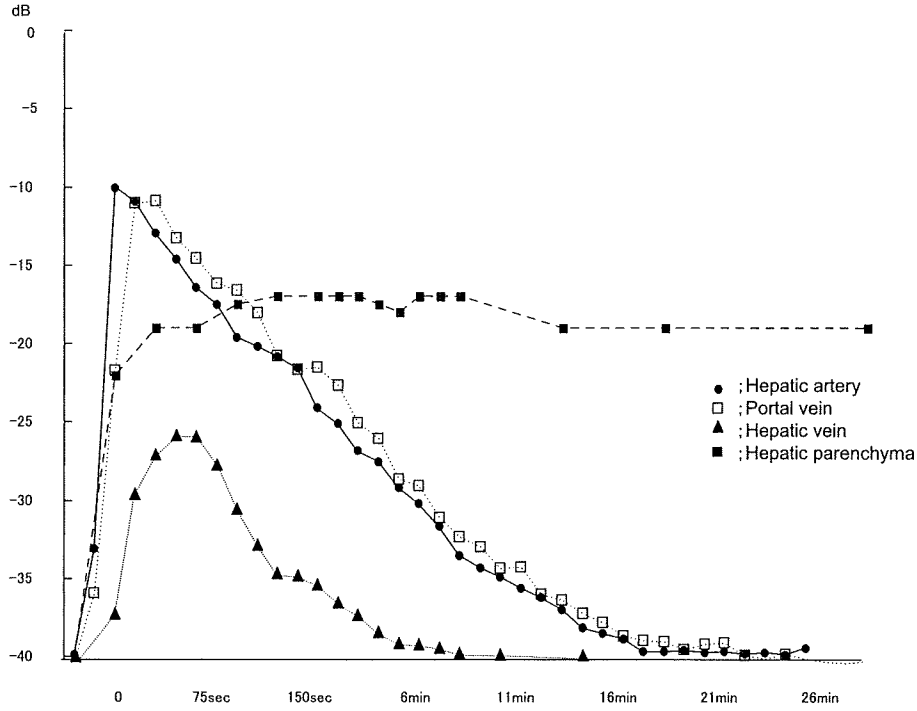

Fig. 1 The Time-Intensity Curves of Sonazoid in healthy volunteers
Sonazoid dosage 0.0075 mg/Kg

された実質造影が得られる．前者は腫瘍血管や血管の狭窄病変を診断するのに使われ，後者は腫瘍の拡がりや臓器の虚血領域を診断するのに使われる．薬理動態から考えると，気泡の血中からの消失は超音波照射による崩壊と血中での自然の崩壊以外では，網内系臓器でのマクロファージによる貪食・崩壊・代謝が主な処理経路である[74)78)]．

Sonazoidは，Levovistと比較してシェルを有するため左心系と右心系での圧の変化による気泡の消失が少ない．従って血中濃度の低下はLevovistより少なく門脈など血管の染影は10分以上続く．LevovistとSonazoid造影剤は，投与されると血中を循環したあと，肝臓や脾臓など網内系へ取り込まれる[76)~78)82)]．実際の健常人にSonazoid造影剤を静注したときの時間信号強度では肝動脈，門脈，肝静脈がピークに達した後，2循環目では肝静脈の染影はほとんどない(Fig. 1)．また肝動脈と門脈の信号強度の差はほとんどなく肝静脈との差が大きいことは類洞に多く溜まり，肝臓ではマクロファージであるKupffer細胞に貪食されていると考えられる[76)~78)82)]．

培養Kupffer細胞におけるin vitroでの検討では，LevovistよりSonazoidの方がKupffer細胞に多く貪食されることが証明されている[76)78)]．

Levovistの代謝経路は，ガラクトース代謝に準ずる．すなわちガラクトースは主に肝臓でグルコースに変換される．ATPの存在下でガラクトースキナーゼによりリン酸化され，次に，ヌクレオチド，UDP-グルコースと反応してUDP-ガラクトースを生じ，UDP-グルコースおよびグルコース-1-リン酸に変化し，さらにグルコースに変換されて糖代謝に入る．その後，ピルビン酸に変換されてクエン酸回路に入った後，水と二酸化炭素に代謝される．排泄経路は，血中に微小気泡が溶解した後消失し，肺から呼気に排泄される[24)]．

Sonazoidのガスは水に難溶性であるperflorobutane (C_4F_{10})であり，未変化のまま呼気中にほぼ全量排泄される．Shellを構成しているのは，リン脂質であるphosphatidyl serineであり，生体内物質と同じ代謝経路で代謝される[83)]．

造影剤の副作用としては，Levovistはガラクトースを使用しておりガラクトース血症の患者では症状が悪化することがあるとされる．Sonazoidは気泡のシェルが卵黄由来の界面活性剤を用いているため卵アレルギー

の患者では症状が発現する恐れがあるとされる．治験段階での副作用の多くは下痢である．2009年1月に集計された使用成績調査によると0.5%の副作用報告があるが重篤なものはない．また，臨床使用されているいずれの造影剤もマイクロバブルの平均粒子径は2～3μmと微小であり，毛細血管への塞栓による副作用の報告はない．しかし急性心筋梗塞など重篤な心疾患や動静脈シャントのある患者では，造影剤が直接左心系に入るため慎重な投与が望ましい．Levovistではin vitroで血小板凝集の報告や，Sonazoidでもラット実験における血小板凝集，また溶血の報告がある[84)～86)]．現時点ではDefinityも含め心電図上の異常や血液尿生化学的検査における重篤な副作用報告はなく[44)86)87)]，さらにSonazoid使用時におけるKupffer細胞の形態異常はおこらないと報告されている[88)]が，造影剤と超音波機器の使用方法を守り安全を考慮し使用するべきと考える．

(2) 音圧

音圧mechanical index（MI）値は，診断用超音波装置での送信音圧のことである．米国やカナダFDAの規制から，眼球（MI値0.23未満）を除き診断用超音波の送信音圧はMI値で1.9未満とされている[89)90)]．通常使用するBモードでの診断用超音波装置のMI値は平均0.7程度とされる[91)]．

超音波造影剤は，診断に適する音圧として高音圧系造影剤と中低音圧系造影剤に大きく分かれる．Levovistは高音圧系造影剤，Sonazoidは中低音圧系造影剤，Optison，SonoVue，Definityは，低音圧系造影剤といえる．高音圧とはMI値でおよそ1.0以上，低音圧とは0.04-0.1程度，Sonazoidはその中間の音圧0.2-0.3で効率よく気泡が共振する[92)～100)]．Sonazoidは，in vitroでMI値1.03を超えると収縮や破壊することが報告されている[88)]．

中低音圧系超音波造影剤の多くは，超音波の照射を受けると容易に共振・崩壊する．この時の信号を映像化するには，組織からの信号を抑え，気泡からのみの信号を映像化することが必要である．照射する音圧を下げていくと，崩壊せず持続的に非線形信号を発して，共振を起こす音圧の閾値巾がある．この性質は，おそらく気泡を形成するshellの性状，とくにshellの弾性に依存していると思われる．一方高音圧系超音波造影剤Levovistは，共振することが少なく，高音圧下で気泡の崩壊の際映像化され，一度崩壊させると以後十分な染影を得ることができない．

(3) 映像技術

従来のドプラ法とは異なる造影法の開発によりLevovistに特化した映像手法が多く開発された．これは，高音圧送信で気泡を崩壊させ，かつ造影感度を向上させ，気泡信号を抽出するなど，非線形信号をより多く取り出せ良好な血流情報が得られ，Levovistに対する感度や空間分解能に優れていた[67)～69)101)]．しかし，リアルタイム性に欠けることや一回の検査しかできないことは変わらぬ最大の欠点であり，また小さな腫瘍では造影剤が崩壊する時の信号の陰により腫瘍診断が困難となることもあった．一方，感度にすぐれるため転移性肝癌や中分化以上の肝細胞癌などKupffer細胞が極めて少ない腫瘍をクリアカットに診断するには適している[69)70)101)]．

Sonazoidなど第2世代の造影超音波検査では，非線形映像法（ハーモニック法）が用いられる．造影性から見ると，一つの気泡が壊れず多くのフレームに亘って映像化されることは，同一気泡数を注射した場合，高音圧で気泡を崩壊して得られる手法に比べて，1フレーム当たりの信号量が大幅に増加することになる．この手法は低音圧ハーモニック法と呼ばれる．

最近の機器では，通常のBモードでもティッシュハーモニック法が用いられていることが多くMI値を下げて造影に用いられることはあるが造影性は悪い．第2世代の造影剤は，前述のように低音圧で気泡を共振させて映像化するのが基本的な手法であるため，パルス波の波数を少なくし，かつ非線形信号の検出に感度の良い手法が望ましい．同時に音圧が低いので，ティッシュハーモニック成分は少ないが，更にそれを低減する手法であるpulse(phase)inversion harmonicに代表される，反転したパルス波を用いる手法が主体となる[102)～106)]．最近では，位相変調法と振幅変調法を駆使して造影剤からの信号を有効に映像化させる手法が出てきているが[107)108)]，Sonazoidのように低音圧といえども少し高い音圧で映像化される造影剤の場合，気泡からの信号か組織からの信号かの区別がつかないことがあり，診断が難渋する場合があり今後さらに機器の進歩が望まれる．

その他，血流情報や血管の形態診断のための情報を得るための手法として低い音圧で送信し，気泡の共振をなるべく長く持続させる，いわゆる低音圧リアルタイム灌流イメージ，やReplenish法，maximum intensity projection（MIP）法などがある[109)～116)]．低音圧リアルタイム灌流イメージでは，低音圧で持続的な実質染影が得られるが血管内の血流からの信号は実質の信号に埋まってしまい，映像化されないため，病変の血

管像が正確に評価できない．Replenish 法は，断層面内を灌流する気泡を，短時間の高い音圧のパルス波によりすべて崩壊消去せしめ，再び低音圧に戻しスキャン面内を再灌流する気泡を映像化するものである．この Replenish 影像法により繰り返し血管造影を得ることができる．低音圧リアルタイム灌流イメージと組み合わせることで肝臓領域では腫瘍の vascularity の多寡を診断し，また再灌流により腫瘍の血流を半定量することが可能となる[116]．MIP 法は，画像ピクセル毎に最高輝度に達した輝度を保持していく手法である．この手法により，1 フレーム毎の血管内のバブルの数がまばらであってもフレームを重ねることにより血管走行が明瞭化する．MIP 法を用いることにより，腫瘍内の分岐して行く細い腫瘍血管の構造も明瞭に描出される．最近の機器にはこれらの機能が搭載され腫瘍新生血管の描出のみならず血管新生阻害剤の治療効果判定などへの応用が期待できる[117)~119)]．

3. 診　断

(1) 肝腫瘍

超音波造影剤による，肝腫瘍診断は多くの報告があり第 1 世代造影剤 Levovist によりその診断は，ほぼ確立されている[120)~128)]．診断のうえでは，造影剤の相違によるに大きな違いはない．しかし第 2 世代超音波造影剤は，中低音圧による映像でリアルタイムに血流診断ができること[48)129)~135)]，また MIP 法を応用した MFI (micro flow imaging) など技術の進歩により詳細な腫瘍血管の形態診断が出来る点で大きく進歩した[111)~114)]．造影超音波における肝腫瘍の鑑別診断のポイントは，血流の多寡と，Sonazoid では，血流情報に加えて肝実質相 (Kupffer phase) による腫瘍と腫瘍周囲の染影の程度，SonoVue や Definity など血管系の造影剤では，late vascular phase による腫瘍部の wash out を観察することにより診断することである[131)]．

多血性肝細胞癌では，造影早期に腫瘍内に流入する腫瘍血管を認める．その後，門脈優位相では，門脈血流の低下を認める事が多い (Fig. 2)．超音波で病変が描出される場合には所謂血管造影に準じた診断が可能である．しかし，Sonazoid の場合，動脈に続いて門脈が造影され引き続き肝実質が染影され Kupffer 細胞の存在が画像に影響していることも念頭に診断する必要がある．SonoVue や Definity のような血管系造影剤が使用できればこの問題は解決できる可能性がある．20 mm 以下の小型肝細胞癌でも多血性のものは同様のパターンをとる[136)]．また，20 mm 以下の乏血性肝細胞癌の場合，造影 CT や MRI で診断困難な場合でも，造影超音波検査で肝細胞癌と診断できることが多く，その場合には肝生検を回避できる点もメリットが大きい[137)~139)]．一方，動脈相が短時間であるため dysplastic nodule など所謂境界病変と鑑別診断には限界があるとの報告もある[140)]．

また，Levovist による肝実質相 (Kupffer phase) による診断は，フェルモデキシスによる造影 MRI と比較的よく相関し，肝細胞癌の分化度との関連もみられる[70)141)]．多くの肝細胞癌の場合，結節部と周囲の肝実質を比較すると不均一な染影の低下となることが多い．Sonazoid でも血管相では同様の所見であるが，高分化型癌，乏血性肝細胞癌や dysplastic nodule など Kupffer 細胞が腫瘍内に存在する腫瘍では 20 分以上経過した時点で肝実質相 (Kupffer phase) の評価をする必要がありそうである．Sonazoid は Levovist より多くの気泡が Kupffer 細胞に貪食されること，肝硬変などの慢性肝疾患では造影剤の再循環が 30 分以上続くことなどによると考えるが現時点での詳細な報告はない．

前述の肝腫瘍の MFI などの血管形態診断や肝実質相 (Kupffer phase) などによる診断は，肝細胞癌や境界病変の鑑別や組織学的悪性度診断に役立つことが報告されている[111)~114)]．

肝癌や転移性肝癌のラジオ波凝固療法などの治療支援や効果判定では，Levovist は一定の評価をされたもののリアルタイム性に乏しく使用に制限があった[123)142)~148)]．しかし治療後の再発部位の同定には高い診断能を示した[71)~73)]．第 2 世代の超音波造影剤では，腫瘍血管を造影剤で確認しながら治療をしたり，Sonazoid では予め造影剤を静注した後に病変部を確認して治療を行う[149)150)]などの方法もあり的確な治療が可能となったことは福音である[149)~152)]．今後は，造影超音波ガイド下に三次元でリアルタイムに腫瘍を穿刺できる可能性もある．単結節周囲増殖型などの肝細胞癌の局所再発を減少できると考える[153)]．

肝血管腫はその特徴から B モードでも鑑別出来ることが多く，カメレオンサイン[154)155)]や B–モードにおける腫瘍内のスペックルのゆらぎ，fluttering signal が特徴的である[156)157)]．基礎疾患に慢性肝炎や肝硬変を合併する場合で腫瘍が高エコーの場合は，脂肪化を伴った早期肝細胞癌との鑑別が必要である．多くの肝血管腫は，vascular phase では造影剤が徐々に腫瘍の周囲から腫瘍内に fill in する様子が経時的に観察される．しかし肝血

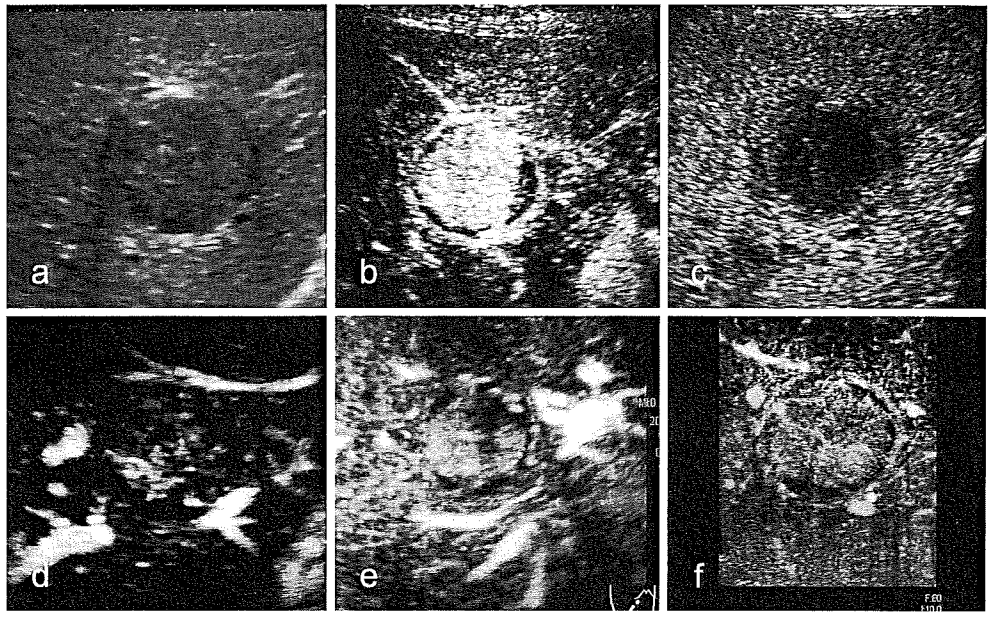

Fig. 2 Contrast-enhanced US images of HCC using Sonazoid
a. Baseline B-mode image shows the mass as a hypoechoic lesion with halo
b. The tumor was stained in the early vascular phase
c. In the Kupffer phase, the tumor area showed hypo intense contrast compared with non-tumor area
d. Tumor vessel by using micro flow imaging (in the early vascular phase)
e. Tumor vessel by using micro flow imaging (in the late vascular phase)
f. Tumor vessel in the tumor were depicted more clearly in the late vascular phase in MFI of intraoperative ultrasound

管腫の組織性状によりその fill in の仕方には若干差が見られる[158]．血管相で特徴ある所見を示すが，造影の経時変化を観察せず肝実質相（Kupffer phase）のみの観察をすると周囲肝実質と比較して染影が低下する場合があり，肝細胞癌と誤る場合があり注意を要する[135)158)159)]．

転移性肝癌の場合は，動脈性の血流は腫瘍中心部で乏しい反面，腫瘍辺縁では hypervascular になることが特徴である．従って腫瘍の中心部が壊死に陥りやすく，vascular phase は造影 CT などの画像診断と同様，動門脈相で腫瘍辺縁に ring 状の染影を認める場合が多い．これは腫瘍周囲の肝組織の門脈枝のつぶれがおこり代償性に動脈血流が増加する事によりおこる．また，造影超音波では，転移性肝細胞癌でも腫瘍が hyper vascular に描出されることが多く，88% が hyper vascular との報告もある[160]．これは造影 CT では，撮像タイミングが固定されているためタイミングに多少のずれが生じ，腫瘍血流がリアルタイムに捉えられていないと考えられる．また，肝実質相（Kupffer phase）では，転移巣は病変部の染影が周囲肝実質と比較すると完全に染影が欠損することが多い．通常の B-モードで検出できない微小転移巣の描出に特に役立つ[161]．

限局性結節性過形成（FNH）は，特に Sonazoid など第2世代の造影超音波検査が診断に有用な肝腫瘍である．腫瘍血管は，遠心性で放射状の血流が特徴であることは言うまでもないが，肝細胞線腫では腫瘍内の不規則な血流が特徴である．両腫瘍の鑑別にも有用であると考える[162)～166)]．FNH は，動脈血が線維性隔壁内の筋性血管から毛細血管を介して線維性隔壁近傍の類洞に注ぎ，類洞内血液は，結節内の類洞を介するか，もしくは直接肝静脈に流出するとされている[167)168)]．肝実質相（Kupffer phase）では，Kupffer 細胞を反映して周囲肝実質とほぼ同等になることが特徴である．

肝腫瘍診断は，腫瘍自体の血流診断のみならず，肝動脈への到達時間を検討することにより肝細胞癌の治療効果判定や転移性肝細胞癌の診断へ応用の報告もある[169)170)]．

(2) びまん性肝疾患

超音波検査は，形態のみならずドプラ法を使った血

流速度の測定という機能診断でも有用であった[171)~173)]．超音波造影剤の使用により気泡の動きを観察することにより類洞の血流評価を行うことができるようになった．これらの造影超音波検査により慢性肝炎から肝硬変へと線維化が進行するにつれ肝静脈への到達時間が短縮すると報告されている[174)~181)]．これは肝内のシャントや肝硬変による全身の循環亢進によることが予想される．肝動脈，門脈などへの到達時間や消失時間の測定は，慢性肝疾患の進展度評価に有用である．また，肝実質染影の時間の程度を肝機能評価に用いることもでき[182)]，超音波造影剤による肝機能評価は，低侵襲的診断法として今後期待される．

近年，メタボリックシンドロームが注目を浴びているが肝臓領域でも脂肪肝から非アルコール性脂肪性肝炎（NASH）を拾い上げる診断法としてLevovist造影超音波検査の有用性が報告されている[183)]．本法は極めて簡便で有用な診断方法であり，NASHのみならず肝臓のKupffer機能診断としても有用であると考えられ，今後アルコール性肝炎や劇症肝炎などの診断に応用できる可能性がある．Kupffer細胞により多く貪食されるSonazoidを使用した定量的Kupffer機能診断などに期待がもたれる．

4. 今後の展望

第2世代超音波造影剤が発売され，1年以上経過した．その一般的な使用方法は，中音圧でバブルを振るわせて診断する．しかし使用方法の工夫の検討もされはじめ，今後臨床面での研究もされるであろう[95)150)]．

肝腫瘍のラジオ波熱凝固療法など局所治療の効果判定は，2次元造影超音波検査においてもその有用性が報告されている．しかし，2次元超音波で腫瘍を穿刺した場合，腫瘍から穿刺針のずれが生じ的確な治療や効果判定ができない．手術や局所療法においては3次元超音波（3D）やリアルタイム3D（4D）による腫瘍の進展，血管の走行などシミュレーションすることにより，的確で安全性の高い治療が行えると考える．しかし，現時点での3Dは，フレームレートが遅くリアルタイム性に乏しい[153)184)~186)]．早急な機器の開発が望まれる．

MFIなど腫瘍の血管新生のイメージは，血管新生阻害剤の治療効果判定に寄与する可能性がある．マウスにおける実験では超音波造影剤が治療効果判定に使用できる可能性も報告されている[117)~119)]．

さらに肝疾患以外の消化器領域の使用法として有用性が高いと考えられるのは，炎症性腸疾患の治療効果判定や炎症の程度の定量的評価は有力である[95)187)188)]．膵癌と腫瘤形成性膵炎の鑑別の有用性は，Levovistでも報告されているが，第2世代の超音波造影剤の登場により内視鏡超音波による鑑別診断などの報告もある[189)~194)]．この分野も高周波で高分解能の機器の開発が必須である．

近年，ナノバブルといわれる1 μm以下の超音波造影剤の開発がされている．これらの造影剤はdrug deliver system（DDS）やgene deliver systemへの応用が研究されている．およそ300 nmから1000 nmの大きさのバブルは，血管外へ流出すると考えられ，腫瘍治療への応用などに期待できるが機器やナノバブルの開発など今後の研究が待たれる[195)196)]．

5. まとめ

造影超音波検査の変遷を中心に肝腫瘍診断および肝機能診断の有用性さらに第2世代の造影剤の特徴について述べた．肝臓領域には造影超音波のみならず多くの有用性の高い診断法があるが，その適応や評価については施設間の差がある．画像が精密になってくるにつれ臨床医は，その画像を理解し駆使することが必ずしも容易ではないからである．各種造影剤の開発と機器の進歩によりますます膨大な知識が要求されるが，超音波診断の利点は簡便かつ低侵襲であり，多くの慢性肝炎を有するわが国では，肝硬変から肝細胞癌を拾い上げるスクリーニングなどにも使用できると考えられる[186)197)]．今後安全性の高い検査法の一つとしてさらに発展する領域であると考える．

文　献

1) Gramiak R, Shah PM, Kramer DH. Ultrasound cardiography: contrast studies in anatomy and function. Radiology 1969; 92: 939—948
2) Feigenba H, Stone JM, Lee DA, et al. Identification of ultrasound echoes from the left ventricle by use of intracardiac injections of indocyanine green. Circulation 1970; 41: 615—621
3) Kerber RE, Dippel WF, Abboud FM. Abnormal motion of the interventricular septum in right ventricular volume overload. Experimental and clinical echocardiographic studies. Circulation 1973; 48: 86—96
4) Kerber RE, Kioschos JM, Lauer RM. Use of an ultrasonic contrast method in the diagnosis of valvu-

lar regurgitation and intracardiac shunts. Am J Cardiol 1974; 34: 722—727
5) Seward JB, Tajik AJ, Spangler JG, et al. Echocardiographic contrast studies: initial experience. Mayo Clin Proc 1975; 50: 163—192
6) Seward JB, Tajik AJ, Hagler DJ, et al. Contrast echocardiography in single or common ventricle. Circulation 1977; 55: 513—519
7) Serruys PW, Vandenbrand M, Hugenholtz PG, et al. Intracardiac right-to-left shunts demonstrated by two-dimensional echocardiography after peripheral vein injection. Br Heart J 1979; 42: 429—437
8) Meltzer RS, Tickner EG, Sahines TP, et al. The source of ultrasound contrast effect. J Clin Ultrasound 1980; 8: 121—127
9) DeMaria AN, Bommer W, Takeda P, et al. Value and limitations of contrast echocardiography in cardiac diagnosis. Cardiovasc Clin 1983; 13: 167—179
10) Klicpera M, Glogar D, Mayr H, et al. Myocardial perfusion evaluated by contrast echocardiography. A preliminary report. Chest 1982; 82: 751—756
11) Munoz S, Berti C, Pulido C, et al. Two-dimensional contrast echocardiography with carbon dioxide in the detection of congenital cardiac shunts. Am J Cardiol 1984; 53: 206—210
12) Matsuda Y, Yabuuchi I. Hepatic tumors: US contrast enhancement with CO_2 microbubbles. Radiology 1986; 161: 701—705
13) Kudo M, Tomita S, Tochio H, et al. Hepatic focal nodular hyperplasia: specific findings at dynamic contrast-enhanced US with carbon dioxide microbubbles. Radiology 1991; 179: 377—382
14) Kudo M, Tomita S, Tochio H, et al. Small hepatocellular carcinoma: diagnosis with US angiography with intraarterial CO_2 microbubbles. Radiology 1992; 182: 155—160
15) Kudo M, Tomita S, Tochio H, et al. Sonography with intraarterial infusion of carbon dioxide microbubbles (sonographic angiography): value in differential diagnosis of hepatic tumors. AJR Am J Roentgenol 1992; 158: 65—74
16) Nomura Y, Matsuda Y, Yabuuchi I, et al. Hepatocellular carcinoma in adenomatous hyperplasia: detection with contrast-enhanced US with carbon dioxide microbubbles. Radiology 1993; 187: 353—356
17) Elmouaaouy A, Naruhn M, Becker HD, et al. Intraoperative echo-contrast ultrasound examination of malignant liver neoplasms—initial clinical experience. Surg Endosc 1991; 5: 214—218
18) Christiansen C, Kryvi H, Sontum PC, et al. Physical and biochemical characterization of Albunex, a new ultrasound contrast agent consisting of air-filled albumin microspheres suspended in a solution of human albumin. Biotechnol Appl Biochem 1994; 19: 307—320
19) Grayburn PA, Weiss JL, Hack TC, et al. Phase III multicenter trial comparing the efficacy of 2% dodecafluoropentane emulsion (EchoGen) and sonicated 5% human albumin (Albunex) as ultrasound contrast agents in patients with suboptimal echocardiograms. J Am Coll Cardiol 1998; 32: 230—236
20) Keller MW, Glasheen W, Kaul S. Albunex: a safe and effective commercially produced agent for myocardial contrast echocardiography. J Am Soc Echocardiogr 1989; 2: 48—52
21) Hilpert PL, Mattrey RF, Mitten RM, et al. IV injection of air-filled human albumin microspheres to enhance arterial Doppler signal: a preliminary study in rabbits. AJR Am J Roentgenol 1989; 153: 613—616
22) Smith MD, Elion JL, McClure RR, et al. Left heart opacification with peripheral venous injection of a new saccharide echo contrast agent in dogs. J Am Coll Cardiol 1989; 13: 1622—1628
23) Schlief R. Ultrasound contrast agents. Curr Opin Radiol 1991; 3: 198—207
24) Uchimoto R, Niwa K, Eguchi H, et al. In vivo kinetics of microbubbles of SHU 508 A (Levovist): Comparison with Indocyanine Green in rabbits. Ultrasound Med Biol 1999; 25: 1365—1370
25) Leen E, Angerson WJ, Warren HW, et al. Improved sensitivity of colour Doppler flow imaging of colorectal hepatic metastases using galactose microparticles: a preliminary report. Br J Surg 1994; 81: 252—254
26) Fujimoto M, Moriyasu F, Nishikawa K, et al. Color Doppler sonography of hepatic tumors with a galactose-based contrast agent: correlation with angiographic findings. AJR Am J Roentgenol 1994; 163: 1099—1104
27) Tanaka S, Kitamra T, Yoshioka F, et al. Effective-

ness of galactose-based intravenous contrast medium on color Doppler sonography of deeply located hepatocellular carcinoma. Ultrasound Med Bio 1995; 21: 157—160

28) Ernst H, Hahn EG, Balzer T, et al. Color Doppler ultrasound of liver lesions: Signal enhancement after intravenous injection of the ultrasound contrast agent Levovist. J Clin Ultrasound 1996; 24: 31—35

29) Sitzer M, Furst G, Siebler M, et al. Usefulness of an intravenous contrast medium in the characterization of high-grade internal carotid stenosis with color Doppler-assisted duplex imaging. Stroke 1994; 25: 385—389

30) Bogdahn U, Frohlich T, Becker G, et al. Vascularization of primary central nervous system tumors: detection with contrast-enhanced transcranial color-coded real-time sonography. Radiology 1994; 192: 141—148

31) Schwarz KQ, Becher H, Schimpfky C, et al. Doppler enhancement with SH U 508A in multiple vascular regions. Radiology 1994; 193: 195—201

32) Bogdahn U, Becker G, Schlief R, et al. Contrast-enhanced transcranial color-coded real-time sonography. Results of a phase-two study. Stroke 1993; 24: 676—684

33) Becker G, Lindner A, Bogdahn U. Imaging of the vertebrobasilar system by transcranial color-coded real-time sonography. J Ultrasound Med 1993; 12: 395—401

34) Suren A, Osmers R, Kulenkampff D, et al. Visualization of blood flow in small ovarian tumor vessels by transvaginal color Doppler sonography after echo enhancement with injection of Levovist. Gynecol Obstet Invest 1994; 38: 210—212

35) Cennamo G, Rosa N, Vallone GF, et al. First experience with a new echographic contrast agent. Br J Ophthalmol 1994; 78: 823—826

36) Otis S, Rush M, Boyajian R. Contrast-enhanced transcranial imaging. Results of an American phase-two study. Stroke 1995; 26: 203—209

37) Missouris CG, Allen CM, Balen FG, et al. Non-invasive screening for renal artery stenosis with ultrasound contrast enhancement. J Hyperten 1996; 14: 519—524

38) Kedar RP, Cosgrove D, McCready VR, et al. Microbubble contrast agent for color Doppler US: Effect on breast masses. Radiology 1996; 198: 679—686

39) Bhutani MS, Hoffman BJ, vanVelse A, et al. Contrast-enhanced endoscopic ultrasonography with galactose microparticles: SHU508 A (Levovist). Endoscopy 1997; 29: 635—639

40) Huber S, Helbich T, Kettenbach J, et al. Effects of a microbubble contrast agent on breast tumors: Computer-assisted quantitative assessment with color Doppler US-Early experience. Radiology 1998; 208: 485—489

41) Postert T, Braun B, Federlein J, et al. Diagnosis and monitoring of middle cerebral artery occlusion with contrast-enhanced transcranial color-coded real-time sonography in patients with inadequate acoustic bone windows. Ultrasound Med Biol 1998; 24: 333—340

42) Claudon M, Plouin PF, Baxter GM, et al. Renal arteries in patients at risk of renal arterial stenosis: Multicenter evaluation of the echo-enhancer SHU 508A at color and spectral Doppler US. Radiology 2000; 214: 739—746

43) Koga M, Kimura K, Minematsu K, et al. Relationship between findings of conventional and contrast-enhanced transcranial color-coded real-time sonography and angiography in patients with basilar artery occlusion. AJNR Am J Neuroradiol 2002; 23: 568—571

44) Kitzman DW, Goldman ME, Gillam LD, et al. Efficacy and safety at the novel ultrasound contrast agent Perflutren (definity) in patients with suboptimal baseline left ventricular echocardiographic images. Am J Cardiol 2000; 86: 669—674

45) Leen E, Angerson WJ, Yarmenitis S, et al. Multicentre clinical study evaluating the efficacy of SonoVue (BR1), a new ultrasound contrast agent in Doppler investigation of focal hepatic lesions. Eur J Radiol 2002; 41: 200—206

46) Krix M, Kiessling F, Essig M, et al. Low mechanical index contrast-enhanced ultrasound better reflects high arterial perfusion of liver metastases than arterial phase computed tomography. Invest Radiol 2004; 39: 216—222

47) Maruyama H, Matsutani S, Saisho H, et al. Different behaviors of microbubbles in the liver: Time-related quantitative analysis of two ultrasound contrast agents, Levovist and Definity. Ultrasound

Med Bio 2004; 30: 1035—1040
48) Gaiani S, Celli N, Piscaglia F, et al. Usefulness of contrast-enhanced perfusional sonography in the assessment of hepatocellular carcinoma hypervascular at spiral computed tomography. J Hepatol 2004; 41: 421—426
49) Ohkusa A, Yoshioka H, Okafuji T, et al. Evaluation of US contrast medium (LEVOVIST) to experimental liver cancer. Nippon Acta Radiologica 1992; 52: 1024—1026
50) Goldberg BB, Liu JB, Burns PN, et al. Galactose-based intravenous sonographic contrast agent: experimental studies. J Ultrasound Med 1993; 12: 463—470
51) Rosenkranz K, Zendel W, Langer R, et al. Contrast-enhanced transcranial Doppler US with a new transpulmonary echo contrast agent based on saccharide microparticles. Radiology 1993; 187: 439—443
52) Kim AY, Choi BI, Kim TK, et al. Hepatocellular carcinoma: Power Doppler US with a contrast agent-Preliminary results. Radiology 1998; 209: 135—140
53) Kamiyama N, Moriyasu F, Mine Y, et al. Analysis of flash echo from contrast agent for designing optimal ultrasound diagnostic systems. Ultrasound Med Biol 1999; 25: 411—420
54) Moriyasu F, Kono Y, Nada T, et al. Flash echo (passive cavitation) imaging of the liver by using US contrast agents and intermittent scanning sequence. Radiology 1996; 201: 374—374
55) Hosten N, Puls R, Lemke AJ, et al. Contrast-enhanced power Doppler sonography: Improved detection of characteristic flow patterns in focal liver lesions. J Clin Ultrasound 1999; 27: 107—115
56) Uggowitzer M, Kugler C, Groll R, et al. Sonographic evaluation of focal nodular hyperplasias (FNH) of the liver with a transpulmonary galactose-based contrast agent (Levovist). Br J Radiol 1998; 71: 1026—1032
57) Bartolozzi C, Lencioni R, Ricci P, et al. Hepatocellular carcinoma treatment with percutaneous ethanol injection: Evaluation with contrast-enhanced color Doppler US. Radiology 1998; 209: 387—393
58) Tanaka S, Kitamra T, Fujita M, et al. Value of contrast-enhanced color Doppler sonography in diagnosing: Hepatocellular carcinoma with special attention to the "color-filled pattern". J Clin Ultrasound 1998; 26: 207—212
59) Fracanzani AL, Burdick L, Borzio M, et al. Contrast-enhanced Doppler ultrasonography in the diagnosis of hepatocellular carcinoma and premalignant lesions in patients with cirrhosis. Hepatology 2001; 34: 1109—1112
60) Kim TK, Han JK, Kim AY, et al. Limitations of characterization of hepatic hemangiomas using a sonographic contrast agent (Levovist) and power Doppler ultrasonography. J Ultrasound Med 1999; 18: 737—743
61) Wu JY, Shung KK. Nonlinear energy exchange among harmonic modes and its applications to nonlinear imaging. J Acoust Soc Am 1990; 88: 2852—2858
62) Ward B, Baker AC, Humphrey VF. Nonlinear propagation applied to the improvement of resolution in diagnostic medical ultrasound. J Acoust Soc Am 1997; 101: 143—154
63) Shapiro RS, Wagreich J, Parsons RB, et al. Tissue harmonic imaging sonography: Evaluation of image quality compared with conventional sonography. AJR Am J Roentgenol 1998; 171: 1203—1206
64) Tranquart F, Grenier N, Eder V, et al. Clinical use of ultrasound tissue harmonic imaging. Ultrasound Med Biol 1999; 25: 889—894
65) Kono Y, Moriyasu F, Nada T, et al. Gray scale second harmonic imaging of the liver: A preliminary animal study. Ultrasound Med Biol 1997; 23: 719—726
66) Kono Y, Moriyasu F, Mine Y, et al. Gray-scale second harmonic imaging of the liver with galactose-based microbubbles. Invest Radiol 1997; 32: 120—125
67) Blomley M, Albrecht T, Cosgrove D, et al. Stimulated acoustic emission imaging ("sono-scintigraphy") with the ultrasound contrast agent Levovist: A reproducible Doppler ultrasound effect with potential clinical utility. Acad Radiol 1998; 5: S236—S239
68) Blomley MJ, Albrecht T, Cosgrove DO, et al. Improved imaging of liver metastases with stimulated acoustic emission in the late phase of enhancement with the US contrast agent SH U 508 A: Early experience. Radiology 1999; 210: 409—416

69) Blomley MJ, Albrecht T, Cosgrove DO, et al. Stimulated acoustic emission to image a late liver and spleen-specific phase of Levovist in normal volunteers and patients with and without liver disease. Ultrasound Med Biol 1999; 25: 1341—1352
70) Suzuki S, Iijima H, Moriyasu F, et al. Differential diagnosis of hepatic nodules using delayed parenchymal phase imaging of levovist contrast ultrasound: comparative study with SPIO-MRI. Hepatol Res 2004; 29: 122—126
71) Youk JH, Lee JM, Kim CS. Therapeutic response evaluation of malignant hepatic masses treated by interventional procedures with contrast-enhanced agent detection imaging. J Ultrasound Med 2003; 22: 911—920
72) Shimizu M, Iijima H, Horibe T, et al. Usefulness of contrast-enhanced ultrasonography with a new contrast mode, Agent Detection Imaging, in evaluating therapeutic response in hepatocellular carcinoma treated with radio-frequency ablation therapy. Hepatol Res 2004; 29: 235—242
73) Kim CK, Choi DG, Lim HK, et al. Therapeutic response assessment of percutaneous radio frequency ablation for hepatocellular carcinoma: Utility of contrast-enhanced agent detection imaging. Eur J Radiol 2005; 56: 66—73
74) Kindberg GM, Tolleshaug H, Roos N, et al. Hepatic clearance of Sonazoid perfluorobutane microbubbles by Kupffer cells does not reduce the ability of liver to phagocytose or degrade albumin microspheres. Cell Tissue Res 2003; 312: 49—54
75) Blomley MJ, Sidhu PS, Cosgrove DO, et al. Do different types of liver lesions differ in their uptake of the microbubble contrast agent SH U 508A in the late liver phase? Early experience. Radiology 2001; 220: 661—667
76) Iijima H, Moriyasu F, Miyahara T, et al. Ultrasound contrast agent, Levovist microbubbles are phagocytosed by Kupffer cells — In vitro and in vivo studies. Hepatol Res 2006; 35: 235—237
77) Yanagisawa K, Moriyasu F, Miyahara T, et al. Phagocytosis of ultrasound contrast agent microbubbles by Kupffer cells. Ultrasound Med Biol 2007; 33: 318—325
78) Watanabe R, Matsumura M, Munemasa T, et al. Mechanism of hepatic parenchyma-specific contrast of microbubble-based contrast agent for ultrasonography-Microscopic studies in rat liver. Invest Radiol 2007; 42: 643—651
79) Maruyama H, Matsutani S, Saisho H, et al. Real-time blood-pool images of contrast enhanced ultrasound with Definity in the detection of tumour nodules in the liver. Br J Radiol 2005; 78: 512—518
80) Schneider M, Arditi M, Barrau MB, et al. BR1: a new ultrasonographic contrast agent based on sulfur hexafluoride-filled microbubbles. Investigative Radiology 1995; 30: 451—457
81) Senior P, Andersson O, Caidahl K, et al. Enhanced left ventricular endocardial border delineation with an intravenous injection of SonoVue, a new echocardiographic contrast agent: A European multicenter study. Echocardiography 2000; 17: 705—711
82) Lim AK, Patel N, Eckersley RJ, et al. Evidence for spleen-specific uptake of a microbubble contrast agent: A quantitative study in healthy volunteers. Radiology 2004; 231: 785—788
83) Uran S, Landmark K, Normann PT, et al. A respiration-metabolism chamber system and a GC-MS method developed for studying exhalation of perfluorobutane in rats after intravenous injection of the ultrasound contrast agent Sonazoid. J Pharm Biomed Anal 2005; 39: 746—751
84) Shigeta K, Taniguchi N, Omoto K, et al. In vitro platelet activation by an echo contrast agent. J Ultrasound Med 2003; 22: 365—373
85) Shigeta K, Itoh K, Ookawara S, et al. The effects of Levovist and DD 723 in activating platelets and damaging hepatic cells of rats. J Ultrasound Med 2005; 24: 967—974
86) ter Haar GR. Ultrasonic contrast agents: safety considerations reviewed. Eur J Radiol 2002; 41: 217—221
87) Landmark KE, Johansen PW, Johnson JA, et al. Pharmacokinetics of perfluorobutane following intravenous bolus injection and continuous infusion of sonazoid in healthy volunteers and in patients with reduced pulmonary diffusing capacity. Ultrasound Med Biol 2008; 34: 494—501
88) Liu GJ, Moriyasu F, Hirokawa T, et al. Optical Microscopic Findings of the Behavior of Perflubutane Microbubbles Outside and Inside Kupffer Cells Du-

ring Diagnostic Ultrasound Examination. Invest Radiol 2008; 43: 829—836
89) Fowlkes JB, Holland CK. Mechanical bioeffects from diagnostic ultrasound: AIUM consensus statements-Introduction. J Ultrasound Med 2000; 19: 69—72
90) Shi WT, Forsberg F. Ultrasonic characterization of the nonlinear properties of contrast microbubbles. Ultrasound Med Biol 2000; 26: 93—104
91) Sheiner E, Freeman J, Abramowicz JS. Acoustic output as measured by mechanical and thermal indices during routine obstetric ultrasound examinations. J Ultrasound Med 2005; 24: 1665—1670
92) Sboros V, Moran CM, Pye SD, et al. The behaviour of individual contrast agent microbubbles. Ultrasound Med Biol 2003; 29: 687—694
93) Miller DL, Averkiou MA, Brayman AA, et al. Bioeffects considerations for diagnostic ultrasound contrast agents. J Ultrasound Med 2008; 27: 611—632
94) Maruyama H, Matsutani S, Saisho H, et al. Greyscale contrast enhancement in rabbit liver with DMP115 at different acoustic power levels. Ultrasound Med Biol 2000; 26: 1429—1438
95) Edey AJ, Ryan SM, Beese RC, et al. Ultrasound imaging of liver metastases in the delayed parenchymal phase following administration of Sonazoid using a destructive mode technique (Agent Detection Imaging. Clin Radiol 2008; 63: 1112—1120
96) Sontum PC, Ostensen J, Dyrstad K, et al. Acoustic properties of NC100100 and their relation with the microbubble size distribution. Invest Radiol 1999; 34: 268—275
97) Emmer M, Vos HJ, Goertz DE, et al. Pressure-dependent attenuation and scattering of phospholipid-coated microbubbles at low acoustic pressures. Ultrasound Med Biol 2009; 35: 102—111
98) Shi WT, Forsberg F, Tornes A, et al. Destruction of contrast microbubbles and the association with inertial cavitation. Ultrasound Med Biol 2000; 26: 1009—1019
99) Forsberg F, Shi WT, Merritt CRB, et al. On the usefulness of the mechanical index displayed on clinical ultrasound scanners for predicting contrast microbubble destruction. J Ultrasound Med 2005; 24: 443—450
100) Cosgrove D. Ultrasound contrast agents: an overview. Eur J Radiol 2006; 60: 324—330
101) Kitamura H, Kawasaki S, Nakajima K, et al. Correlation between microbubble contrast-enhanced color Doppler sonography and immunostaining for Kupffer cells in assessing the histopathologic grade of hepatocellular carcinoma: Preliminary results. J Clin Ultrasound 2002; 30: 465—471
102) Burns PN, Wilson SR, Simpson DH. Pulse inversion imaging of liver blood flow: improved method for characterizing focal masses with microbubble contrast. Invest Radiol 2000; 35: 58—71
103) Albrecht T, Hoffmann CW, Schettler S, et al. B-mode enhancement at phase-inversion US with air-based microbubble contrast agent: Initial experience in humans. Radiology 2000; 216: 273—278
104) Kim AY, Choi BI, Kim TK, et al. Comparison of contrast-enhanced fundamental imaging, second-harmonic imaging, and pulse-inversion harmonic imaging. Investigative Radiology 2001; 36: 582—588
105) Wilson SR, Burns PN. An algorithm for the diagnosis of focal liver masses using microbubble contrast-enhanced pulse-inversion sonography. AJR Am J Roentgenol 2006; 186: 1401—1412
106) Wilson SR, Burns PN. Liver mass evaluation with ultrasound: The impact of microbubble contrast agents and pulse inversion imaging. Semin Liver Dis 2001; 21: 147—159
107) Eckersley RJ, Chin CT, Burns PN. Optimising phase and amplitude modulation schemes for imaging microbubble contrast agents at low acoustic power. Ultrasound Med Biol 2005; 31: 213—219
108) Leavens C, Williams R, Foster FS, et al. Golay pulse encoding for microbubble contrast imaging in ultrasound. IEEE Trans Ultrason Ferroelectr Freq Control 2007; 54: 2082—2090
109) Porter TR, Oberdorfer J, Rafter P, et al. Microbubble responses to a similar mechanical index with different real-time perfusion imaging techniques. Ultrasound Med Biol 2003; 29: 1187—1192
110) Wei K, Jayaweera AR, Firoozan S, et al. Quantification of myocardial blood flow with ultrasound-induced destruction of microbubbles administered as a constant venous infusion. Circulation 1998; 97: 473—483
111) Muradali D, Kulkarni SR, Villet C, et al. Angiogenesis mapping with pulse inversion: A new and sensitive method to image vascularity in breast carcino-

mas. Radiology 2002; 225: 367—367
112) Wilson SR, Jang HJ, Kim TK, et al. Real-time temporal maximum-intensity-projection imaging of hepatic lesions with contrast-enhanced sonography. AJR Am J Roentgenol 2008; 190: 691—695
113) Yang H, Liu GJ, Lu MD, et al. Evaluation of the vascular architecture of hepatocellular carcinoma by micro flow imaging-Pathologic correlation. J Ultrasound Med 2007; 26: 461—467
114) Sugimoto K, Moriyasu F, Kamiyama N, et al. Analysis of morphological vascular changes of hepatocellular carcinoma by microflow imaging using contrast-enhanced sonography. Hepatol Res 2008; 38: 790—799
115) Sehgal CM, Cary TW, Arger PH, et al. Delta-projection Imaging on Contrast-enhanced Ultrasound to Quantify Tumor Microvasculature and Perfusion. Acad Radiol 2009; 16: 71—78
116) Sugimoto K, Moriyasu F, Kamiyama N, et al. Correlation between parametric imaging using contrast ultrasound and the histological differentiation of hepatocellular carcinoma. Hepatol Res 2008; 38: 273—280
117) Willmann JK, Paulmurugan R, Chen K, et al. US imaging of tumor angiogenesis with microbubbles targeted to vascular endothelial growth factor receptor type 2 in mice. Radiology 2008; 246: 508—518
118) Kruskal JB. Can contrast-enhanced US with targeted microbubbles monitor the response to antiangiogenic therapies? Radiology 2008; 246: 339—340
119) Lavisse S, Lejeune P, Rouffiac V, et al. Early quantitative evaluation of a tumor vasculature disruptive agent AVE8062 using dynamic contrast-enhanced ultrasonography. Invest Radiol 2008; 43: 100—111
120) Harvey CJ, Blomley MJ, Eckersley RJ, et al. Pulse-inversion mode imaging of liver specific microbubbles: improved detection of subcentimetre metastases. Lancet 2000; 355: 807—808
121) Kim TK, Choi BI, Han JK, et al. Hepatic tumors: Contrast agent-enhancement patterns with pulse-inversion harmonic US. Radiology 2000; 216: 411—417
122) Choi BI, Kim TK, Han JK, et al. Vascularity of hepatocellular carcinoma: Assessment with contrast-enhanced second-harmonic versus conventional power Doppler US. Radiology 2000; 214: 381—386
123) Ding H, Kudo M, Onda H, et al. Evaluation of post-treatment response of hepatocellular carcinoma with contrast-enhanced coded phase-inversion harmonic US: Comparison with dynamic CT. Radiology 2001; 221: 721—730
124) Celik H, Ozdemir H, Yucel C, et al. Characterization of hyperechoic focal liver lesions-Quantitative evaluation with pulse inversion harmonic imaging in the late phase of Levovist. J Ultrasound Med 2005; 24: 39—47
125) Ogawa S, Kumada T, Toyoda H, et al. Evaluation of pathological features of hepatocellular carcinoma by contrast-enhanced ultrasonography: Comparison with pathology on resected specimen. Eur J Radiol 2006; 59: 74—81
126) Hotta N, Tagaya T, Maeno T, et al. Advanced dynamic flow Imaging with contrast-enhanced ultrasonography for the evaluation of tumor vascularity in liver tumors. Clin Imaging 2005; 29: 34—41
127) Kobayashi S, Maruyama H, Okugawa H, et al. Contrast-enhanced US with Levovist for the diagnosis of hepatic hemangioma: Time-related changes of enhancement appearance and the hemodynamic background. Hepatogastroenterology 2008; 55: 1222—1228
128) Brannigan M, Burns P, Wilson S. Blood flow patterns in focal liver lesions at microbubble-enhanced US. Radiographics 2004; 24: 921—935
129) Wilson SR, Burns PN, Muradali D, et al. Harmonic hepatic US with microbubble contrast agent: Initial experience showing improved characterization of hemangioma, hepatocellular carcinoma, and metastasis. Radiology 2000; 215: 153—161
130) Basilico R, Blomley MJ, Harvey CJ, et al. Which continuous US scanning mode is optimal for the detection of vascularity in liver lesions when enhanced with a second generation contrast agent? Eur J Radiol 2002; 41: 184—191
131) Jang HJ, Kim TK, Burns PN, et al. Enhancement patterns of hepatocellular carcinoma at contrast-enhanced US: comparison with histologic differentiation. Radiology 2007; 244: 898—906
132) Giorgio A, Ferraioli G, Tarantino L, et al. Contrast-enhanced sonographic appearance of hepatocellular carcinoma in patients with cirrhosis: Compari-

son with contrast-enhanced helical CT appearance. AJR Am J Roentgenol 2004; 183: 1319—1326

133) Ding H, Wang WP, Huang BJ, et al. Imaging of focal liver lesions-Low-mechanical-index real-time ultrasonography with SonoVue. J Ultrasound Med 2005; 24: 285—297

134) Ricci P, Laghi A, Cantisani V, et al. Contrast-enhanced sonography with SonoVue: Enhancement patterns of benign focal liver lesions and correlation with dynamic gadobenate dimeglumine-enhanced MRI. AJR Am J Roentgenol 2005; 184: 821—827

135) Celli N, Gaiani S, Piscaglia F, et al. Characterization of liver lesions by real-time contrast-enhanced ultrasonography. Eur J Gastroenterol Hepatol 2007; 19: 3—14

136) Jang HJ, Kim TK, Wilson SR. Small nodules (1-2 cm) in liver cirrhosis: Characterization with contrast-enhanced ultrasound. Eur J Radiol 2008 sep.

137) Dai Y, Chen MH, Fan ZH, et al. Diagnosis of small hepatic nodules detected by surveillance ultrasound in patients with cirrhosis: Comparison between contrast-enhanced ultrasound and contrast-enhanced helical computed tomography. Hepatol Res 2008; 38: 281—290

138) Forner A, Vilana R, Ayuso C, et al. Diagnosis of hepatic nodules 20 mm or smaller in cirrhosis: Prospective validation of the noninvasive diagnostic criteria for hepatocellular carcinoma. Hepatology 2008; 47: 97—104

139) Yoshizumi H, Maruyama H, Okugawa H, et al. How to characterize non-hypervascular hepatic nodules on contrast-enhanced computed tomography in chronic liver disease: feasibility of contrast-enhanced ultrasound with a microbubble contrast agent. J Gastroenterol Hepatol 2008; 23: 1528—1534

140) Lencioni R, Piscaglia F, Bolondi L. Contrast-enhanced ultrasound in the diagnosis of hepatocellular carcinoma. J Hepatol 2008; 48: 848—857

141) Inoue T, Kudo M, Watai R, et al. Differential diagnosis of nodular lesions in cirrhotic liver by post-vascular phase contrast-enhanced US with Levovist: comparison with superparamagnetic iron oxide magnetic resonance images. J Gastroenterol 2005; 40: 1139—1147

142) Choi D, Lim HK, Kim SH, et al. Hepatocellular carcinoma treated with percutaneous radio-frequency ablation: Usefulness of power Doppler US with a microbubble contrast agent in evaluating therapeutic response-preliminary results. Radiology 2000; 217: 558—563

143) Solbiati L, Goldberg SN, Ierace T, et al. Radio-frequency ablation of hepatic metastases: Postprocedural assessment with a US microbubble contrast agent-Early experience. Radiology 1999; 211: 643—649

144) Liu JB, Goldberg BB, Merton DA, et al. The role of contrast-enhanced sonography for radiofrequency ablation of liver tumors. J Ultrasound Med 2001; 20: 517—523

145) Cioni D, Lencioni R, Rossi S, et al. Radiofrequency thermal ablation of hepatocellular carcinoma: Using contrast-enhanced harmonic power Doppler sonography to assess treatment outcome. Am J Roentgenol 2001; 177: 783—788

146) Choi D, Lim HK, Lee WJ, et al. Early assessment of the therapeutic response to radio frequency ablation for hepatocellular carcinoma-Utility of gray scale harmonic ultrasonography with a microbubble contrast agent. J Ultrasound Med 2003; 22: 1163—1172

147) Wen YL, Kudo M, Zheng RQ, et al. Radiofrequency ablation of hepatocellular carcinoma: Therapeutic response using contrast-enhanced coded phase-inversion harmonic sonography. AJR Am J Roentgenol 2003; 181: 57—63

148) Meloni MF, Goldberg SN, Livraghi T, et al. Hepatocellular carcinoma treated with radiofrequency ablation: Comparison of pulse inversion contrast-enhanced harmonic sonography, contrast-enhanced power Doppler sonography, and helical CT. AJR Am J Roentgenol 2001; 177: 375—380

149) 工藤正俊，畑中絹世，鄭　浩柄，他．肝細胞癌治療支援における Sonazoid 造影エコー法の新技術の提唱　Defect Re-perfusion Imaging の有用性．肝臓 2007；48：299—301

150) Numata K, Morimoto M, Ogura T, et al. Ablation therapy guided by contrast-enhanced sonography with Sonazoid for hepatocellular carcinoma lesions not detected by conventional sonography. J Ultrasound Med 2008; 27: 395—406

151) Chen MH, Wu W, Yang W, et al. The use of

contrast-enhanced ultrasonography in the selection of patients with hepatocellular carcinoma for radio frequency ablation therapy. J Ultrasound Med 2007; 26: 1055—1063

152) Solbiati L, Ierace T, Tonolini M, et al. Guidance and monitoring of radiofrequency liver tumor ablation with contrast-enhanced ultrasound. Eur J Radiol 2004; 51: S19—S23

153) Leen E, Kumar S, Khan S, et al. Contrast-enhanced 3D ultrasound in the radiofrequency ablation of liver tumors. World J Gastroenterol 2009; 15: 289—299

154) 大竹宏治, 朝井　均, 池岡直子. 体位変換による肝血管腫の超音波像の変化("Chameleon" Sign) についての検討. 日本画像医学雑誌　1991；10：120—125

155) Tsujimoto F, Abe T, Murakami Y, et al. Temporal changes in internal echoes in hepatic hemangiomas. Nippon Acta Radiologica 1989; 49: 574—582

156) 竹内和男. 肝血管腫の超音波像　拡大及び dynamic image による観察.「日本超音波医学会研究発表会講演論文集」(44 回). 1984；319—320

157) 飯島尋子, 肥塚明日香, 松岡弘高, 他. 肝血管腫にみられるスペックルのゆらぎ"fluttering signal"について. 超音波医学　2000；27：457

158) Dietrich C, Mertens J, Braden B, et al. Contrast-enhanced ultrasound of histologically proven liver hemangiomas. Hepatology 2007; 45: 1139—1145

159) Wilson SR, Kim TK, Jang HJ, et al. Enhancement patterns of focal liver masses: discordance between contrast-enhanced sonography and contrast-enhanced CT and MRI. AJR Am J Roentgenol 2007; 189: W7—W12

160) Murphy-Lavallee J, Jang HJ, Kim TK, et al. Are metastases really hypovascular in the arterial phase? The perspective based on contrast-enhanced ultrasonography. J Ultrasound Med 2007; 26: 1545—1556

161) Piscaglia F, Corradi F, Mancini M, et al. Real time contrast enhanced ultrasonography in detection of liver metastases from gastrointestinal cancer. Bmc Cancer 2007; 7

162) Attal P, Vilgrain V, Brancatelli G, et al. Telangiectatic focal nodular hyperplasia: US, CT, and MR imaging findings with histopathologic correlation in 13 cases. Radiology 2003; 228: 465—472

163) Iijima H, Suzuki S, Moriyasu F, et al. Visualization of the drainage veins with contrast-enhanced sonography was useful in diagnosis of small focal nodular hyperplasia. J Ultrasound Med 2006; 25: 799—803

164) Dietrich CF, Schuessler G, Trojan J, et al. Differentiation of focal nodular hyperplasia and hepatocellular adenoma by contrast-enhanced ultrasound. Br J Radiol 2005; 78: 704—707

165) Kim TK, Jang HJ, Burns PN, et al. Focal nodular hyperplasia and hepatic adenoma: Differentiation with low-mechanical-index contrast-enhanced sonography. AJR Am J Roentgenol 2008; 190: 58—66

166) Yen YH, Wang JH, Lu SN, et al. Contrast-enhanced ultrasonographic spoke-wheel sign in hepatic focal nodular hyperplasia. Eur J Radiol 2006; 60: 439—444

167) Fukukura Y, Nakashima O, Kusaba A, et al. Angioarchitecture and blood circulation in focal nodular hyperplasia of the liver. Journal of Hepatology 1998; 29: 470—475

168) Wanless IR, Mawdsley C, Adams R. On the pathogenesis of focal nodular hyperplasia of the liver. Hepatology 1985; 5: 1194—1200

169) Zhou X, Strobel D, Haensler J, et al. Hepatic transit time: indicator of the therapeutic response to radiofrequency ablation of liver turnours. Br J Radiol 2005; 78: 433—436

170) Zhou JH, Li AH, Cao LH, et al. Haemodynamic parameters of the hepatic artery and vein can detect liver metastases: assessment using contrast-enhanced ultrasound. Br J Radiol 2008; 81: 113—119

171) Moriyasu F, Ban N, Nishida O, et al. Quantitative measurement of portal blood flow in patients with chronic liver disease using an ultrasonic Duplex system consisting of a pulsed Doppler flowmeter and B-mode electroscanner. Gastroenterol Jpn 1984; 19: 529—536

172) Moriyasu F, Nishida O, Ban N, et al. Measurement of portal vascular resistance in patients with portal hypertension. Gastroenterology 1986; 90: 710—717

173) Hamato N, Moriyasu F, Someda H, et al. Clinical application of hepatic venous hemodynamics by Doppler ultrasonography in chronic liver disease. Ultrasound Med Biol 1997; 23: 829—835

174) Albrecht T, Blomley MJ, Cosgrove DO, et al. Non-invasive diagnosis of hepatic cirrhosis by transit-

time analysis of an ultrasound contrast agent. Lancet 1999; 353: 1579—1583
175) Bang N, Nielsen MB, Rasmussen AN, et al. Hepatic vein transit time of an ultrasound contrast agent: simplified procedure using pulse inversion imaging. Br J Radiol 2001; 74: 752—755
176) Blomley MJ, Lim AK, Harvey CJ, et al. Liver microbubble transit time compared with histology and Child-Pugh score in diffuse liver disease: a cross sectional study. Gut 2003; 52: 1188—1193
177) Lim AK, Taylor-Robinson SD, Patel N, et al. Hepatic vein transit times using a microbubble agent can predict disease severity non-invasively in patients with hepatitis C. Gut 2005; 54: 128—133
178) Lim AK, Patel N, Eckersley RJ, et al. Hepatic vein transit time of SonoVue: A comparative study with Levovist. Radiology 2006; 240: 130—135
179) Ridolfi F, Abbattista T, Marini F, et al. Contrast-enhanced ultrasound to evaluate the severity of chronic hepatitis C. Dig Liver Dis 2007; 39: 929—935
180) Searle J, Mendelson R, Zelesco M, et al. Non-invasive prediction of the degree of liver fibrosis in patients with hepatitis C using an ultrasound contrast agent. A pilot study. J Med Imaging Radiat Oncol 2008; 52: 130—133
181) Blomley MJ, Albrecht H, Cosgrove DO, et al. Liver vascular transit time analyzed with dynamic hepatic venography with bolus injections of an US contrast agent: Early experience in seven patients with metastases. Radiology 1998; 209: 862—866
182) Maruyama H, Matsutani S, Okugawa H, et al. Microbubble disappearance-time is the appropriate timing for liver-specific imaging after injection of levovist. Ultrasound Med Biol 2006; 32: 1809—1815
183) Iijima H, Moriyasu F, Tsuchiya K, et al. Decrease in accumulation of ultrasound contrast microbubbles in non-alcoholic steatohepatitis. Hepatol Res 2007; 37: 722—730
184) Arita J, Kokudo N, Zhang KM, et al. Three-dimensional visualization of liver segments on contrast-enhanced intraoperative sonography. AJR Am J Roentgenol 2007; 188: W464—W466
185) Xu HX, Lu MD, Xie XH, et al. Three-dimensional contrast-enhanced ultrasound of the liver: Experience of 92 cases. Ultrasonics 2008
186) Rahbin N, Siosteen AK, Elvin A, et al. Detection and characterization of focal liver lesions with contrast-enhanced ultrasonography in patients with hepatitis C-induced liver cirrhosis. Acta Radiol 2008; 49: 251—257
187) Kratzer W, Schmidt SA, Mittrach C, et al. Contrast-enhanced wideband harmonic imaging ultrasound (SonoVue): A new technique for quantifying bowel wall vascularity in Crohn's disease. Scand J Gastroenterol 2005; 40: 985—991
188) Serra C, Menozzi G, Labate AMM, et al. Ultrasound assessment of vascularization of the thickened terminal ileum wall in Crohn's disease patients using a low-mechanical index real-time scanning technique with a second generation ultrasound contrast agent. Eur J Radiol 2007; 62: 114—121
189) Tawada K, Yamaguchi T, Kobayashi A, et al. Changes in tumor vascularity depicted by contrast-enhanced ultrasonography as a predictor of chemotherapeutic effect in patients with unresectable pancreatic cancer. Pancreas 2009; 38: 30—35
190) Dietrich C, Ignee A, Braden B, et al. Improved differentiation of pancreatic tumors using contrast-enhanced endoscopic ultrasound. Clin Gastroenterol Hepatol 2008; 6: 590—597
191) Kitano M, Sakamoto H, Matsui U, et al. A novel perfusion imaging technique of the pancreas: contrast-enhanced harmonic EUS (with video). Gastrointest Endosc 2008; 67: 141—150
192) Itoh T, Hirooka Y, Itoh A, et al. Usefulness of contrast-enhanced transabdominal ultrasonography in the diagnosis of intraductal papillary mucinous tumors of the pancreas. Am J Gastroenterol 2005; 100: 144—152
193) Kitano M, Kudo M, Maekawa K, et al. Dynamic imaging of pancreatic diseases by contrast enhanced coded phase inversion harmonic ultrasonography. Gut 2004; 53: 854—859
194) Sofuni A, Iijima H, Moriyasu F, et al. Differential diagnosis of pancreatic tumors using ultrasound contrast imaging. J Gastroenterol 2005; 40: 518—525
195) Zheng HR, Mukdadi S, Shandas R. Theoretical predictions of harmonic generation from submicron ultrasound contrast agents for nonlinear biomedical ultrasound imaging. Phys Med Biol 2006; 51: 557—573
196) Couture O, Bevan PD, Cherin E, et al. Investigating

perfluorohexane particles with high-frequency ultrasound. Ultrasound Med Biol 2006; 32: 73—82
197) Lanka B, Jang HJ, Kim TK, et al. Impact of contrast-enhanced ultrasonography in a tertiary clinical practice. J Ultrasound Med 2007; 26: 1703—1714

Contrast-enhanced ultrasound in the diagnosis of liver diseases —Tracing the history and Perspective—

Hiroko Iijima*

Key words: contrast ultrasound　liver diseases　liver tumor　Kupffer image　microbubble

Kanzo 2009; 50: 105—121

Ultrasound Imaging Center, Division of Hepatobiliary and Pancreatic Diseases Department of Internal Medicine Hyogo College of Medicine
*Corresponding author: hiroko-i@hyo-med.ac.jp

J Gastroenterol 2009; 44:228–235
DOI 10.1007/s00535-008-2304-4

Journal of Gastroenterology

Involvement of hepatoma-derived growth factor in the growth inhibition of hepatocellular carcinoma cells by vitamin K_2

Teruhisa Yamamoto, Hideji Nakamura, Weidong Liu, Ke Cao, Shohei Yoshikawa, Hirayuki Enomoto, Yoshinori Iwata, Noritoshi Koh, Masaki Saito, Hiroyasu Imanishi, Soji Shimomura, Hiroko Iijima, Toshikazu Hada, and Shuhei Nishiguchi

Division of Hepatobiliary and Pancreatic Medicine, Department of Internal Medicine, Hyogo College of Medicine, 1-1 Mukogawa-cho, Nishinomiya, Hyogo 663-8501, Japan

Background. Vitamin K_2 has been reported to suppress the growth of human hepatocellular carcinoma (HCC) in vitro and hepatocarcinogenesis in hepatitis C virus (HCV)-related cirrhosis in vivo. Hepatoma-derived growth factor (HDGF) is a unique nuclear targeting growth factor that is highly expressed in HCC cells and is a possible prognostic factor for patients with HCC. We investigated the regulation of HDGF expression by vitamin K_2. ***Methods.*** Three HCC-derived cell lines, HepG2, HuH-7, and SK-Hep-1, were used. Cell number was determined with the MTT assay. The expression levels of HDGF mRNA and protein were measured by the real-time reverse transcriptase-polymerase chain reaction (PCR) method and ELISA and Western blot analysis, respectively. The HDGF promoter activity was measured by a dual luciferase-reporter assay. ***Results.*** Vitamin K_2 suppressed the growth of the three HCC cell lines in a dose-dependent manner. Vitamin K_2 significantly suppressed the expression of the HDGF protein and mRNA in three cell lines. By a luciferase assay, vitamin K_2 significantly suppressed the promoter activity of the HDGF protein. Based on some luciferase-reporter plasmids containing truncated promoter regions, the possible responsive site of vitamin K_2 seems to reside in the region −1 to −150 bp of the HDGF gene. ***Conclusions.*** These findings suggested that regulation of the HDGF gene expression is one of the crucial mechanisms of vitamin K_2-induced cell growth suppression for HCC.

Key words: HDGF, HCC, vitamin K_2, luciferase assay

Introduction

Hepatoma-derived growth factor (HDGF) is a unique nuclear targeting growth factor with heparin affinity that was purified and cloned from a human hepatocellular carcinoma (HCC) cell line.[1–4] HDGF has both oncogenic and angiogenic activity.[5,6] HDGF stimulates the proliferation of HCC cells, in addition to fibroblasts, endothelial cells, vascular smooth muscle cells, and fetal hepatocytes, after translocation to the nucleus by use of the bipartite nuclear localization signals.[1–9] HDGF is highly expressed in several cancers including HCC and is closely related to the aggressive biological potential of cancer cells.[10–16] A downregulation of HDGF by antisense oligonucleotides or siRNA treatment suppresses the proliferation of cancer cells that express HDGF endogenously.[14,17] Recently, a significant correlation has been shown between HDGF expression and the prognosis for the recurrence-free and overall survival in patients with HCC.[18,19] HDGF is considered to play an important role in both hepatocarcinogenesis and cancer progression. If HDGF expression is suppressed by drugs or chemical agents, then the growth of HCC cells should be regulated efficiently. However, the regulation mechanism of HDGF expression has not yet been clarified.

Vitamin K, an essential hydrophobic vitamin, and its derivatives have been shown to inhibit the proliferation of cancer cells including HCC.[20–23] However, the precise mechanism of their growth inhibitory action has not yet been clarified. Vitamin K consists of different forms, vitamin K_1–K_5. Vitamin K_2 (menaquinone) is produced by the intestinal flora and is used as an oral medication for patients with osteoporosis. The in vivo preventive effect of vitamin K_2 on the development of HCC, or the recurrence after treatment of HCC, in patients with HCV-related cirrhosis has been reported.[24,25] Recent in vitro studies have advocated some molecular mechanisms for the growth inhibition by vitamin K_2: a pathway

Received: February 21, 2008 / Accepted: September 27, 2008
Reprint requests to: H. Nakamura

via protein kinase A activation, induction of the cell cycle-regulating proteins including p21, and reduced expression of the cyclin-dependent kinases.[26–29] However, these mechanisms cannot explain the entire suppressive effects of vitamin K_2 on the proliferation of HCC cells. Other unknown mechanisms have been suggested for the cell proliferation inhibitory effects of vitamin K. The transcriptional regulation of the growth factor genes or growth factor receptor genes by vitamin K_2 has not yet been reported.

In the present study, we investigated the regulation of HDGF expression by vitamin K_2 in HCC cells.

Materials and methods

Materials

Vitamin K_2 (menatetrenone, MK-4) was supplied from Eisai Co. (Tokyo, Japan). The human HCC cell lines HepG2, HuH-7, and SK-Hep-1 were purchased from American Type Culture Collection (ATCC). These cell lines were cultured in Dulbecco's modified Eagle's essential medium (DMEM; Gibco BRL, Grand Island, NY, USA) with 10% fetal bovine serum (FBS), penicillin (100 units/ml), and streptomycin (100 μg/ml) at 37°C in a humidified incubator with 5% CO_2.

Cell proliferation assays

The cells were seeded onto 96-well plates at a density of 2.5×10^3 cells. After a 24-h culture, 100 μl fresh medium containing different concentrations of vitamin K_2 (10, 30, and 100 μM) was added in each well. Vitamin K_2 was dissolved in 99% ethanol at the concentration of 10 mM and then diluted with DMEM to the appropriate concentrations for the experiments. Forty-eight hours later, the culture medium was replaced with fresh medium containing different concentrations of vitamin K_2. The control cells were cultured in DMEM containing the corresponding concentration of ethanol to each dose of the vitamin K_2. After a 4-day culture with vitamin K_2 treatment, the number of viable cells in each well was determined with the 3-(4,5-dimethyl-2-thiazolyl-2,5-diophenyl-2*H*-tetrazolium bromide) (MTT) assay (Roche, Nutley, NJ, USA) according to the manufacturer's instructions.

All experiments were carried out in four wells concurrently, and then were repeated three times.

Western blotting

After a 96-h culture with vitamin K_2, the cells were washed twice with ice-cold phosphate-buffered saline (PBS), lysed, and sonicated in RIPA buffer [1× PBS, 1% Nonidet P-40, 0.5% sodium deoxycholate, 0.1% sodium dodecyl sulfate (SDS), 100 μg/ml phenylmethylsulfonyl fluoride, 45 μg/ml aprotinin, 100 mM sodium orthovanadate]. The supernatant of the homogenate was used for protein determination with a BCA Protein Assay Kit (Pierce, Rockford, IL, USA) and electrophoresis. The samples with 5 μg total protein were electrophoresed on a 12.5% SDS-polyacrylamide gel under reducing conditions and blotted to a polyvinylidene difluoride (PVDF) membrane by electroblotting. The membranes were blotted with the anti-C terminus of the HDGF polyclonal antibody at a dilution of 1:10000, which was generated by the New Zealand White rabbit.[3] The signals were developed with an ABC kit (Vector, Burlingame, CA, USA) and diaminobenzidine.

HDGF-overexpressing HepG2 cells

We constructed *myc*-tagged human HDGF in pEF-BOS plasmids and selected and cloned stable transfectants after transfection to HepG2 as described previously.[3]

HDGF-knock-down SK-Hep-1 cells by shRNA

SuperSilencing shRNA plasmid for human HDGF was purchased from SuperArray Bioscience Corporation (catalog number: KH10419N). SK-Hep-1 was seeded at 1×10^5 cells in 6-well plates with 2 ml 10% FBS-DMEM medium. Next day, 2 μg HDGF-shRNA and the negative control shRNA plasmids were transfected into the cells by 5.0 μl Lipofectamine 2000, according to the protocol from SuperArray. The transfected medium was changed by 10% FBS-DMEM with Geneticin (G418), 1200 mg/l, after 24 h. The G418 media were changed every 3 days. The knock-down expression of HDGF protein was confirmed by Western blot in SK-Hep-1 cells selected by G418 media.

A quantitative reverse transcription-polymerase chain reaction (RT-PCR) analysis of HDGF mRNA levels

HDGF mRNA expression was measured by a quantitative real-time PCR according to the method previously reported.[18] In brief, the total RNA was extracted with the AGPC method using Isogen (Nippongene, Tokyo, Japan); 5 μg deoxyribonuclease I-treated total RNA was used for the reverse transcriptase reaction. An aliquot representing 100 ng input RNA was amplified by using a TaqMan PCR Reagent Kit (Applied Biosystems, Foster City, CA, USA) with the ABI PRISM 7700 sequence Detection System (Applied Biosystems) as follows: 50°C for 2 min, 95°C for 10 min, and 40 cycles at 95°C for 15 s, and 60°C for 1 min. The forward primer 5′-AAGTTTGGCAAGCCCAACA-3′, reverse primer 5′-GGCTCTTCCACACAGCTCTTT-3′, and probe

5′-FAM-AACCCTACTGTCAAGGCTTCCGGCT-TAMRA-3′ were used for HDGF. As an internal control, beta-actin mRNA was used. The RNA extracted from HuH-7 cells was used as a standard. After reverse transcription (RT), standard complementary DNA (cDNA) was serially diluted to obtain five standard solutions for use in the PCR reaction to generate the reference curve. The relative amount of cDNA in each sample was measured by the interpolation of the standard curve, and then the relative ratio of the HDGF/beta-actin expression was calculated for each sample.

Luciferase assay of HDGF promoter activity

Constructs of luciferase-reporter plasmids of the HDGF promoter region. The DNA from the HuH-7 cells was extracted by the Isogen method. Thereafter, the DNA was digested by Tth111 I, purified by phenol/chloroform, and precipitated by ethanol. The HDGF promoter DNA was acquired by a nested PCR. First, 0.5 μg digested and purified DNA was amplified by the forward primer HDGF P5F5 (5′-TACGACATCAGGAGTTCG AAACCA-3′) and the reverse primer HDGF P3R (5′-TGCGCGCTCGTCGAGTTGTTTGT-3′) using a LA TAKARA Taq Kit (RR002A) (Takara, Kyoto, Japan). This PCR product was used as the template of the second amplification. The second PCR was done by series primer pairs designed by DNASIS software using a TAKARA Taq Kit. The DNA amplification was performed in the condition of 94°C for 1 min, 55°C for 1 min, and 72°C for 1 min, for 35 cycles.

Plasmid constructs

The PCR products were purified, polished, and inserted into the pGL3 Basic luciferase-reporter vector predigested by *Sma*I, and transfected into *Escherichia coli* by a PCR Cloning Kit (Stratagene, La Jolla, CA, USA), according to the manufacturer's instructions. The isolated plasmids containing the desired HDGF promoters were verified by *Kpn*I plus *Xho*I digestions and sequenced using the RV Primer 3 from the 5′-end and the GL Primer 2 from the 3′-end.

Luciferase assay of luciferase-reporter plasmids

The HepG2 cells (2×10^5 cells/well) were seeded in a 6-well culture dish (Iwaki, Funabashi, Chiba, Japan) in phenol red-free DMEM containing 5% charcoal-dextran-stripped fetal bovine serum (FBS-CCS). The cells were transfected with 2 μg luciferase-reporter vectors by using a Fugene 6 transfection reagent kit (Roche), according to the manufacturer's recommendations. Twenty-four hours later, the culture media were changed to the fresh media with several concentrations (0, 10, 30, and 100 μM) of vitamin K_2. After incubation for 24 h, the cells were harvested and lysed with luciferase lysis buffer (Promega, Madison, WI, USA). The proteins were measured by a BCA protein assay kit. The luciferase activity of each sample was measured by a luciferase assay kit (Promega). The level of induction was calculated by dividing the mean luciferase activity of the samples treated with vitamin K_2 by the mean activity of the untreated control samples. All experiments were carried out in triplicate and repeated at least three times.

Enzyme-linked immunosorbent assay (ELISA) of HDGF protein

The cells were lysed with the RIPA buffer, as described above. After centrifugation at 10000 rpm for 30 min, the supernatants of the cell lysate were used for the measurement of the HDGF protein by an ELISA. An ELISA for the HDGF was developed by the sandwich method using a monoclonal antibody and a polyclonal antibody against HDGF.

Statistical analysis

The results are expressed as the means ± SE. At least three separate experiments were performed for each data point. The statistical analyses were done using Student's unpaired *t* test (two tailed).

Results

Effect of vitamin K_2 on HCC cells

In patients whom vitamin K_2 are administered at clinically used doses, the serum concentration is calculated to reach to about 30 μM. Thus, we used three doses—10, 30, and 100 μM—of vitamin K_2 in the subsequent experiments. Vitamin K_2 suppressed the proliferation of three HCC cell lines in a dose-dependent manner. The inhibitory effects by vitamin K_2 after 96 h treatment at 30 μM and 100 μM are shown for the three HCC cell lines in Fig. 1.

HDGF was expressed in three cell lines (Fig. 2a). The intracellular HDGF amounts in these cell lines were measured by an ELISA (Fig. 2b). HCC cells with higher production of the HDGF protein seem to show higher inhibition of HCC cell proliferation by vitamin K_2, although not significantly. Some growth factors are involved in the proliferation of HCC cells. Next, we knocked down the HDGF expression and assessed its participating level on the proliferation of HCC cells. We obtained two stable HDGF-knock-down clones after transfection of HDGF-shRNA into SK-Hep-1 cells. In

two SK-Hep-1 clones, of which HDGF expressions were stably knock-downed 64% and 40%, their proliferation was significantly suppressed, but partially at about 35% and 11%, in clone 1 (HDGF-shRNA1) and clone 3 (HDGF-shRNA3), respectively (Fig. 2c). Thus, HDGF is partly involved in the proliferation of HCC cells.

Effect of vitamin K_2 on HDGF protein expression in HCC cells

HDGF protein in the HuH-7 cells decreased after vitamin K_2 treatment by a Western blot analysis (data not shown). By the use of an ELISA for HDGF, we measured intracellular levels of HDGF protein in three HCC cell lines after vitamin K_2 treatment for 96 h. The vitamin K_2 treatment significantly suppressed the HDGF protein expression on three HCC cell lines (Fig. 3).

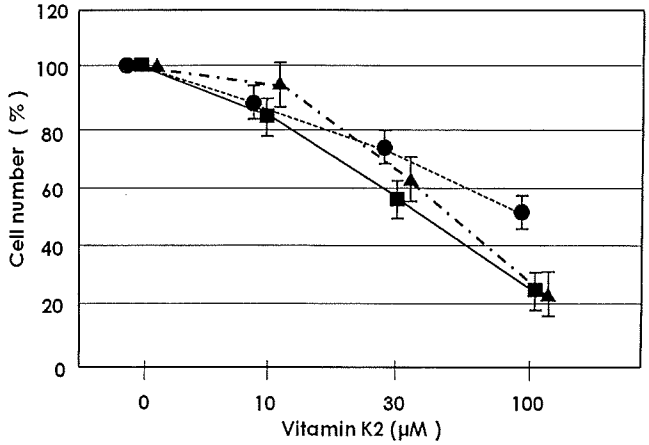

Fig. 1. Vitamin K_2 suppressed the proliferation of human hepatocellular cells dose-dependently. HepG2 (●), HuH-7 (▲), and SK-Hep-1 (■) were treated with various concentrations of vitamin K_2. After vitamin K_2 treatment for 96 h, the cell numbers were determined by the MTT method. Data are mean ± SE of three independent experiments

Recovery of vitamin K_2-induced suppression of HCC proliferation by overexpression of HDGF

Next, we investigated the restorative effect of HDGF on the suppression of HCC cell proliferation by vitamin K_2 by use of HDGF-overexpressing HepG2 cells. The overexpression of HDGF significantly recovered the vitamin K_2-induced suppression of HepG2 cell proliferation, but partially, about 50% (Fig. 4). Thus, these findings suggest that the suppression of HDGF expression is one pathway of vitamin K_2-mediated growth inhibitory mechanisms in HCC cells.

Effect of vitamin K_2 on HDGF mRNA expression

HDGF mRNA expression was measured by a quantitative real-time PCR method. In the HepG2, HuH-7, and SK-Hep-1 cells, HDGF mRNA expression was suppressed 36.5%, 39.5%, and 22.5%, respectively, after vitamin K_2 treatment for 96 h at the dose of 30 μM. The HDGF mRNA expression was suppressed by vitamin K_2 at 51.1%, 63.3%, and 66.2% in the HepG2, HuH-7, and SK-Hep-1 cells, respectively, at the dose of 100 μM (Fig. 5). Next, we investigated whether vitamin K_2 suppressed the promoter activity of HDGF by a dual luciferase assay. It is difficult to transfect plasmids to HuH-7 cells, and we examined this reporter assay in the other two HCC cell lines. In the HepG2 and SK-Hep-1 cells, vitamin K_2 significantly suppressed the luciferase

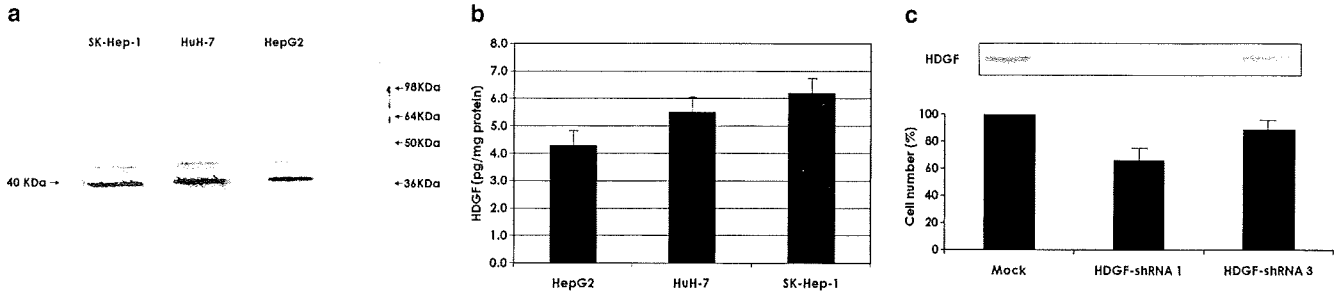

Fig. 2. Expression of hepatoma-derived growth factor (HDGF) protein in human HCC cell lines. Three HCC cell lines were lysed and vortexed with lysis buffer after 48 h culture. After centrifugation, the supernatants of each cell line were used for analysis. **a** Western blot analysis. The cell lysate with 5 μg protein from each cell line was loaded and electrophoresed. After electroblotting, the membrane was blotted with anti-HDGF antibody (C-terminus) at a dilution of 1:10000. **b** Intracellular HDGF protein by an enzyme-linked immunosorbent assay (ELISA). The cell lysates after centrifugation were analyzed in an ELISA kit for HDGF. Data are mean ± SE of three independent experiments. **c** Knock-down of HDGF expression suppressed the proliferation of SK-Hep-1 cells. The stably HDGF-knock-down SK-Hep-1 clones (HDGF-shRNA1 and -3) and mock cells were cultured for 96 h, and then cell numbers were measured by MTT assay. HDGF protein expression in each clone was shown by Western blot

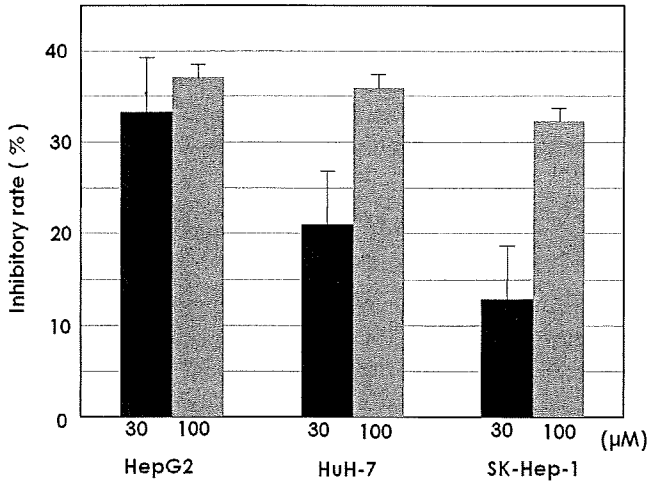

Fig. 3. HDGF protein expression in HCC cells was suppressed by vitamin K_2. Inhibitory rate of HDGF protein expression by vitamin K_2 is shown. Three HCC cell lines were treated with vitamin K_2 at the dose of 30 μM or 100 μM for 96 h. The HCC cells were lysed and vortexed with lysis buffer, and the cell lysates after centrifugation were analyzed by an ELISA kit for HDGF. The data are shown as the mean ± SE of three independent experiments

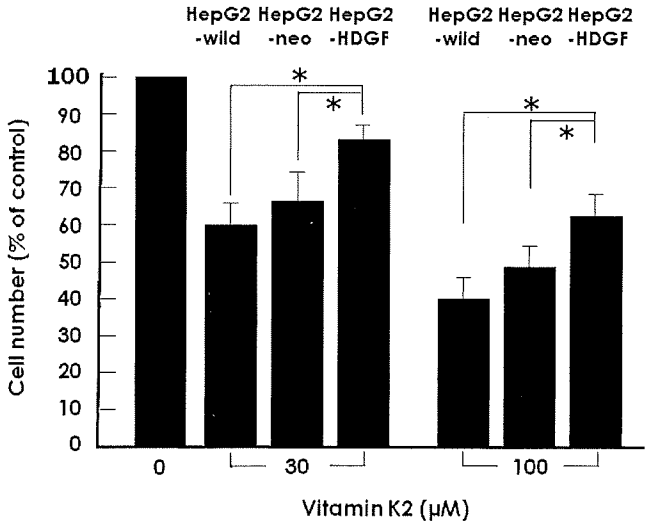

Fig. 4. HDGF overexpression recovered the vitamin K_2-induced suppression of cell proliferation. HDGF-overexpressing HepG2 (HepG2-HDGF), mock (HepG2-neo), and parent HepG2 (HepG2-wild) cells were treated with 30 or 100 μM vitamin K_2. Ninety-six hours later, cell numbers of each well were measured by MTT assay. $^*P < 0.05$

activity by 47.7% and 86.9%, respectively, at 30 μM vitamin K_2 after transfection of the H2 promoter (Fig. 6). The luciferase activity was suppressed 78.2% and 97.0% in the HepG2 and SK-Hep-1 cells at the dose of 100 μM, respectively. Therefore, vitamin K_2 significantly suppressed the gene expression of HDGF in the HCC cells.

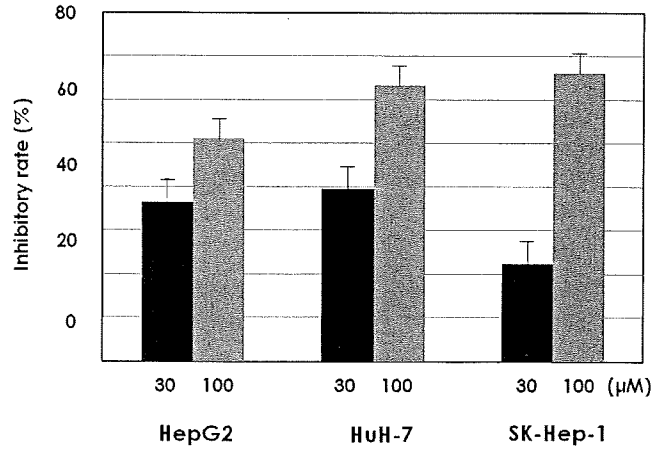

Fig. 5. HDGF mRNA expression was suppressed by vitamin K_2. Three HCC cell lines were treated with vitamin K_2 at 30 μM or 100 μM for 96 h. After RNA extraction, HDGF mRNA expression was measured by the quantitative real-time PCR method. The data are shown as the mean ± SE of three independent experiments

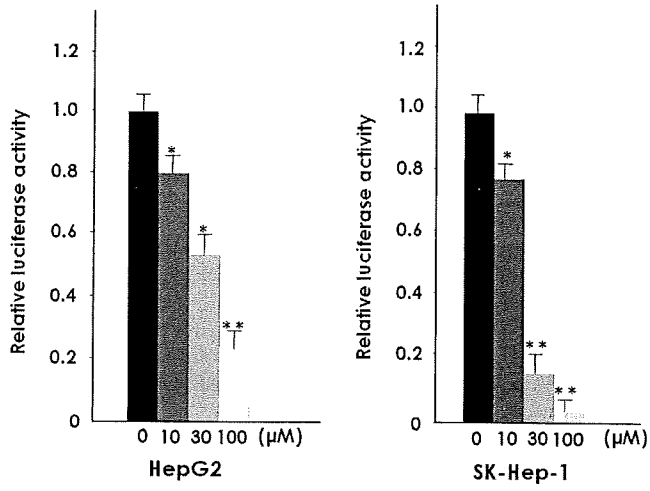

Fig. 6. Vitamin K_2 suppressed the transcription of HDGF. HepG2 and SK-Hep-1 were transfected with 1 μg promoter vector (pLuc-H2). After incubation with the indicated concentrations (μM) of vitamin K_2 for 24 h, the cells were harvested and the relative luciferase activities were measured. The data are shown as the mean ± SE of three independent experiments. $^*P < 0.05$; $^{**}P < 0.01$ vs. control

Possible interaction site of vitamin K_2 in the promoter of the HDGF gene

Next, we constructed the luciferase-reporter plasmids including a truncated promoter region (Fig. 7a). The luciferase activity of the H2 promoter was significantly suppressed in the SK-Hep-1 cells, but that of H12 or -13 was not (Fig. 7b). Therefore, the interaction site of vitamin K_2 seems to reside in the region −1 to −150 bp of the HDGF gene. These findings suggest that the sup-